AMERICAN SOCIETY FOR MICROBIOLOGY | Journal of Bacteriology®

RESEARCH ARTICLE

Identification and Characterization of a Novel *pic* Gene Cluster Responsible for Picolinic Acid Degradation in *Alcaligenes faecalis* JQ135

Jiguo Qiu,[a] Lingling Zhao,[a] Siqiong Xu,[a] Qing Chen,[a,c] Le Chen,[a] Bin Liu,[a] Qing Hong,[a] Zhenmei Lu,[b] Jian He[a]

[a]Key Laboratory of Agricultural Environmental Microbiology, Ministry of Agriculture, College of Life Sciences, Nanjing Agricultural University, Nanjing, China
[b]College of Life Sciences, Zhejiang University, Hangzhou, China
[c]College of Life Sciences, Zaozhuang University, Zaozhuang, China

ABSTRACT Picolinic acid (PA) is a natural toxic pyridine derivative. Microorganisms can degrade and utilize PA for growth. However, the full catabolic pathway of PA and its physiological and genetic foundation remain unknown. In this study, we identified a gene cluster, designated *picRCEDFB4B3B2B1A1A2A3*, responsible for the degradation of PA from *Alcaligenes faecalis* JQ135. Our results suggest that PA degradation pathway occurs as follows: PA was initially 6-hydroxylated to 6-hydroxypicolinic acid (6HPA) by PicA (a PA dehydrogenase). 6HPA was then 3-hydroxylated by PicB, a four-component 6HPA monooxygenase, to form 3,6-dihydroxypicolinic acid (3,6DHPA), which was then converted into 2,5-dihydroxypyridine (2,5DHP) by the decarboxylase PicC. 2,5DHP was further degraded to fumaric acid through PicD (2,5DHP 5,6-dioxygenase), PicE (*N*-formylmaleamic acid deformylase), PicF (maleamic acid amidohydrolase), and PicG (maleic acid isomerase). Homologous *pic* gene clusters with diverse organizations were found to be widely distributed in *Alpha-*, *Beta-*, and *Gammaproteobacteria*. Our findings provide new insights into the microbial catabolism of environmental toxic pyridine derivatives.

IMPORTANCE Picolinic acid is a common metabolite of L-tryptophan and some aromatic compounds and is an important intermediate in organic chemical synthesis. Although the microbial degradation/detoxification of picolinic acid has been studied for over 50 years, the underlying molecular mechanisms are still unknown. Here, we show that the *pic* gene cluster is responsible for the complete degradation of picolinic acid. The *pic* gene cluster was found to be widespread in other *Alpha-*, *Beta-*, and *Gammaproteobacteria*. These findings provide a new perspective for understanding the catabolic mechanisms of picolinic acid in bacteria.

KEYWORDS *Alcaligenes faecalis*, bacterial degradation, pathway, *pic* gene cluster, picolinic acid

Picolinic acid (PA) is a dead-end metabolite of L-tryptophan via the kynurenine pathway in humans and other mammals (1, 2). It is often detected in various biological media, such as cell culture supernatants, serum, and human milk (3). PA can also be produced through other biological processes, such as the microbial degradation of 2-aminophenol, nitrobenzene, catechol, anthranilic acid, and 3-hydroxyanthranilic acid (4–7) (see Fig. S1 in the supplemental material). Furthermore, PA is an important intermediate in the organic synthesis of pharmaceuticals (e.g., carbocaine), herbicides (e.g., picloram and diquat), and fungicides (e.g., 3-trifluoromethyl picolinic acid) (8, 9). Due to its chelating properties, PA has also been added to chromium and iron preparations to treat diabetes and anemia (10, 11). Nevertheless, many studies have shown that PA is highly toxic to organisms. PA inhibits the growth of normal rat kidney cells and the proliferation of T cells, enhances seizure activity in mice, and

Citation Qiu J, Zhao L, Xu S, Chen Q, Chen L, Liu B, Hong Q, Lu Z, He J. 2019. Identification and characterization of a novel *pic* gene cluster responsible for picolinic acid degradation in *Alcaligenes faecalis* JQ135. J Bacteriol 201:e00077-19. https://doi.org/10.1128/JB.00077-19.

Editor William W. Metcalf, University of Illinois at Urbana Champaign

Address correspondence to Jian He, hejian@njau.edu.cn.

Received 25 January 2019
Accepted 30 May 2019
Accepted manuscript posted online 3 June 2019
Published 24 July 2019

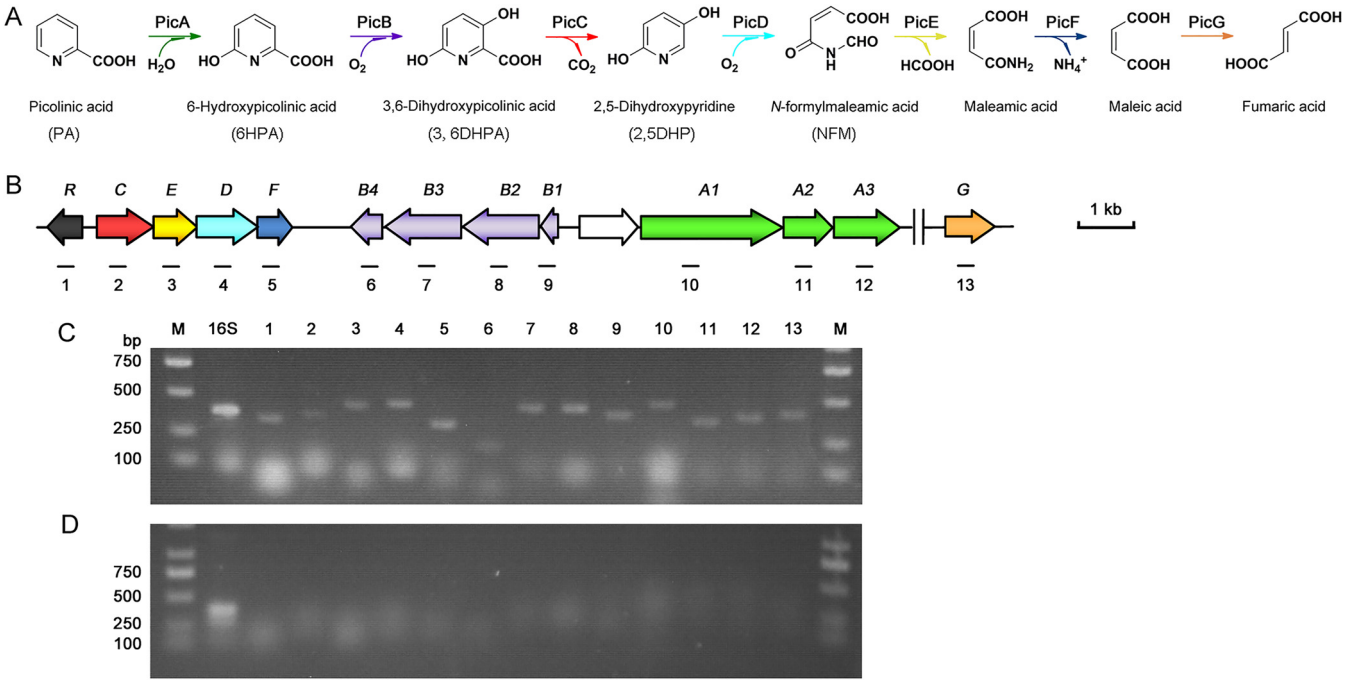

FIG 1 PA degradation in *A. faecalis* JQ135. (A) The proposed PA catabolic pathway and corresponding enzymes. (B) Genetic organization of the *pic* gene cluster. Genes are annotated according to the color scheme in panel A. (C and D) Agarose gel electrophoresis of RT-PCR products generated using RNA of *A. faecalis* JQ135 cells grown with PA (C) or citrate (D). Lane M, DNA marker; lane 16S, positive control. Lanes 1 to 13 correspond to the regions marked in panel B.

induces cell death via apoptosis (12–14). In particular, PA showed high antimicrobial activity at concentrations as low as 8 μg/liter (15–17).

PA cannot be metabolized in the human body and is excreted through urine or sweat (18). Nevertheless, many microorganisms, such as *Alcaligenes* (19), *Arthrobacter* (20), *Burkholderia* (21), and *Streptomyces* (22), and an unidentified Gram-negative bacterium (designated the UGN strain) were shown to degrade PA (23). Through identification of metabolites, a bacterial degradation pathway for PA was proposed (Fig. 1): PA is 6-hydroxylated to 6-hydroxypicolinic acid (6HPA), which is 3-hydroxylated to 3,6-dihydroxypicolinic acid (3,6DHPA), which is further decarboxylated to 2,5-dihydroxypyridine (2,5DHP), a central degradation intermediate of many pyridine derivatives (24, 25). However, little is known about this catabolic pathway at genetic level.

In our previous studies, the bacterial strain *Alcaligenes faecalis* JQ135 was isolated from municipal wastewater and was shown to efficiently degrade and utilize PA (26, 27). A mutant of strain JQ135 that was unable to grow on PA was screened through random transposon mutagenesis (28). Bioinformatic analysis indicated that the transposon was inserted into a gene designated *picC*. PicC was found to be a decarboxylase that catalyzes the decarboxylation of 3,6DHPA to 2,5DHP, which is the third step in PA degradation (28). However, the complete catabolic pathway of PA and its underlying genetic foundation are still unknown. In this study, we found that *picC* is located within the *pic* gene cluster (Fig. 1), and the function of each gene in this cluster was identified via *in vitro* enzymatic assays and gene disruption. In addition, the distribution and organization of *pic* clusters in other bacteria were also investigated.

RESULTS AND DISCUSSION

Identification of a gene cluster involved in PA degradation. Previous studies have shown that the 3,6DHPA decarboxylase PicC was involved in PA metabolism (28). In this study, we investigated the genes located upstream and downstream of *picC* through bioinformatic analysis. The results showed that *picC* was located in a gene cluster (designated *pic*) (Fig. 1), consisting of 12 genes, including a putative regulatory

TABLE 1 The *pic* genes and assigned functions in *Alcaligenes faecalis* JQ135

Gene (locus tag)	Product (aa)[a]	Assigned function	Sequence identity (%)	Homologous protein in UniProtKB/SwissProt (accession no.)
picR (*AFA_15150*)	186	MarR-type negative regulator PicR	33	MexR (P52003)
picC (*AFA_15145*)	323	3,6DHPA decarboxylase	37	2,3-Dihydroxybenzoate decarboxylase (P80402)
picE (*AFA_15140*)	274	*N*-Formylmaleamic acid deformylase	60	NFM deformylase (Q88FY3)
picD (*AFA_15135*)	350	2,5DHP 5,6-dioxygenase	55	2,5-DHP dioxygenase (Q88FY1)
picF (*AFA_15130*)	216	Maleamic acid amidohydrolase	43	Maleamic acid amidohydrolase (Q88FY5)
picB4 (*AFA_15125*)	172	6HPA monooxygenase subunit IV	35	Anthranilate 1,2-dioxygenase small subunit (Q84BZ2)
picB3 (*AFA_15120*)	429	6HPA monooxygenase subunit III	45	Salicylate 5-hydroxylase, oxygenase large subunit (O52379)
picB2 (*AFA_15115*)	425	6HPA monooxygenase subunit II	36	Benzene 1,2-dioxygenase ferredoxin reductase (B1LNJ8)
picB1 (*AFA_15110*)	104	6HPA monooxygenase subunit I	46	Naphthalene 1,2-dioxygenase ferredoxin (Q51493)
picA1 (*AFA_15100*)	800	PA dehydrogenase large subunit	39	Caffeine dehydrogenase large subunit (D7REY3)
picA2 (*AFA_15095*)	278	PA dehydrogenase small subunit	33	Carbon monoxide dehydrogenase medium chain (P19914)
picA3 (*AFA_15090*)	395	PA dehydrogenase medium subunit	46	Carbon monoxide dehydrogenase small chain (P19915)
picG (*AFA_16520*)	253	Maleic acid *cis-trans* isomerase	99	Maleic acid isomerase (O24766)

[a]aa, amino acid.

gene *picR* and 11 putative catabolic genes (*picA1*, *picA2*, *picA3*, *picB1*, *picB2*, *picB3*, *picB4*, *picC*, *picE*, *picD*, and *picF*). The predicted functions of these genes are summarized in Table 1. Reverse transcription-PCR (RT-PCR) analysis showed that all of the *pic* genes were induced by PA but not by citrate (Fig. 1). The above results strongly suggested that the *pic* cluster was involved in PA catabolism in *A. faecalis* JQ135.

The *picA1A2A3* genes encode the PA dehydrogenase (PicA). Previous studies have reported that PA was initially 6-hydroxylated to 6HPA (19, 23, 27, 29). The hydroxylation of *N*-heterocyclic aromatic compounds is usually catalyzed by multicomponent molybdopterin-containing dehydrogenases (30, 31). In the *pic* gene cluster, the *picA1*, *picA2*, and *picA3* gene products showed the highest similarities (~40%) to the respective subunits of three-component molybdopterin-containing dehydrogenases, such as the carbon monoxide dehydrogenase and caffeine dehydrogenase (Table 1). PicA1 and PicA2 were predicted to contain binding domains for the molybdopterin cytosine dinucleotide (MCD) and flavin adenine dinucleotide (FAD), respectively, and PicA3 contained two predicted [Fe-S] clusters (Fig. 2). Thus, *picA1*, *picA2*, and *picA3* were predicted to encode a three-component molybdopterin-containing dehydrogenase that catalyzes the initial step in the PA catabolic pathway. When *picA1A2A3* were deleted, the resulting mutant JQ135 Δ*picA1A2A3* lost the ability to grow on PA but could still grow on 6HPA (see Fig. S2 in the supplemental material). The complemented strain JQ135 Δ*picA1A2A3*/pBBR-*picA1A2A3* regained the ability to grow on PA. Moreover, the *picA1A2A3* genes were then cloned into pBBR1MCS-5 (pBB-*picA1A2A3*) and transferred into *Pseudomonas putida* KT2440, which does not degrade PA, 6HPA, and 3,6DHPA (30). High-performance liquid chromatography (HPLC) results showed that the recombinant KT/pBBR-*picA1A2A3* strain acquired the ability to convert 1 mM PA into approximately equivalent amounts of 6HPA (Fig. 3). Liquid chromatography-time of flight mass spectrometry (LC/TOF-MS) analysis also showed that the product was 6HPA {the molecular ion peak ($[M+H]^+$) 140.0345}. When lacking one component, the recombinants KT/pBBR-*picA2A3* and KT/pBBR-*picA1A2* did not show the conversion ability (data not shown), indicating that all of the three components were essential.

To investigate the PA dehydrogenase activity of KT/pBBR-*picA1A2A3*, the recombinant strain was cultured in mineral salts medium (MSM) containing 1.0 mM citrate and 1.0 mM PA for 12 h, and the cell lysate of KT/pBBR-*picA1A2A3* was tested for PA dehydrogenase activity with phenazine methosulfate (PMS) as an electron acceptor. The K_m value for PA at pH 7.0 and 25°C was 0.65 ± 0.14 μM, and the V_{max} was 44.89 ± 2.45 mU/mg (Fig. S3). No PA dehydrogenase activity was detected under anaerobic conditions, which was similar to results for the nicotinate hydroxylase (NicAB) in *P. putida* KT2440 (30). All of these results demonstrated that the *picA1A2A3* genes are responsible for the hydroxylation of PA to 6HPA in *A. faecalis* JQ135.

The *picB1B2B3B4* genes encode a four-component 6HPA monooxygenase (PicB). The second step in PA catabolism is predicted to be the 3-hydroxylation of 6HPA

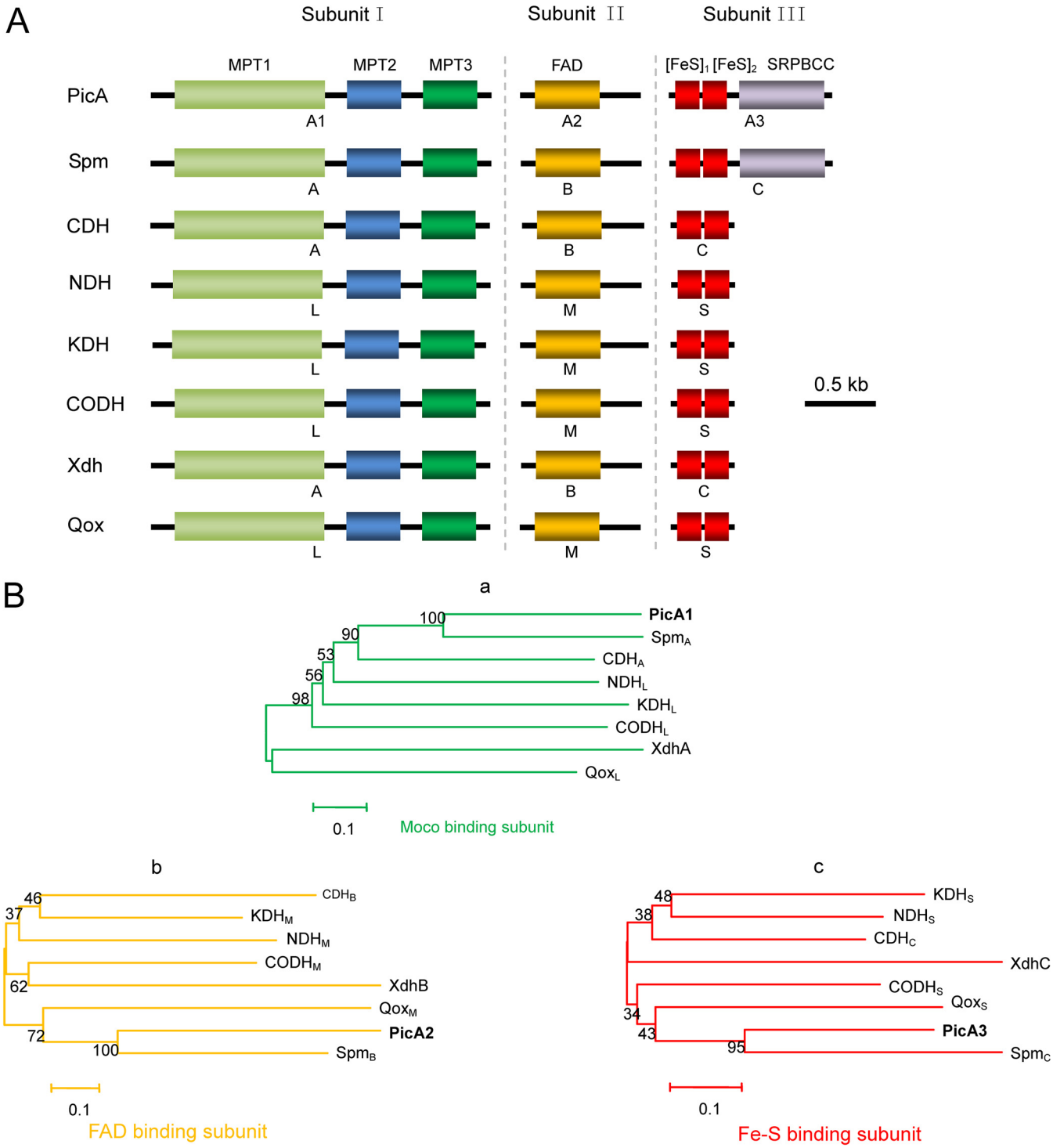

FIG 2 Bioinformatic analysis of PicA. (A) Molecular architecture of several multicomponent molybdenum-containing hydroxylases. Subunits I, II, and III are molybdopterin cytosine dinucleotide (MCD)-, FAD-, and two [Fe-S] cluster-containing components, respectively. Spm_{ABC} (GenBank accession numbers AEJ14617 and AEJ14616), 3-succinoylpyridine dehydrogenase from *P. putida*; CDH_{ABC} (D7REY3, D7REY4, and D7REY5), caffeine dehydrogenase from *Pseudomonas* sp. strain CBB1; NDH_{LMS} (CAA53088, CAA53087, and CAA53086), nicotine dehydrogenase from *Arthrobacter nicotinovorans*; KDH_{LMS} (WP_016359451, WP_016359456, and WP_016359457), ketone dehydrogenase from *A. nicotinovorans*; $CODH_{LMS}$ (P19913, P19914, and P19915), carbon monoxide dehydrogenase from *Hydrogenophaga pseudoflava*; XDH_{ABC} (Q46799, Q46800, and Q46801), xanthine dehydrogenase from *E. coli*; Qox_{LMS} (CAD61045, CAD61046, and CAD61047), quinaldine 4-oxidase from *Arthrobacter ilicis*. The letters depicted below the proteins indicate the subunit names of the corresponding proteins. The conserved domains are as follows: MPT, domain for binding to the molybdopterin cytosine dinucleotide cofactor (MoCo); FAD, FAD-binding domain; [FeS], ferredoxin-like [2Fe-2S]-binding domain; SRPBCC, SRPBCC ligand-binding domain. (B) Phylogenetic analysis of PicA and related molybdenum-containing hydroxylases: PicA1 and the Moco binding subunit of other enzymes (a); PicA2 and the FAD binding subunit of other enzymes (b); PicA3 and the [2Fe-2S] binding subunit of other enzymes (c). The phylogenetic trees were constructed by using the neighbor-joining method (with a bootstrap of 1,000) with software MEGA, version 6.0. The bar represents the number of amino acid substitutions per site.

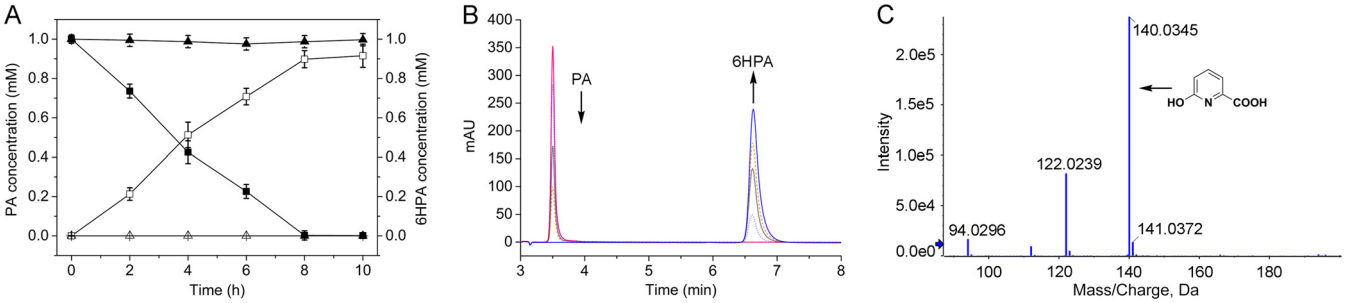

FIG 3 Conversion of PA into 6HPA by recombinant strain KT/pBBR-*picA1A2A3*. (A) The time course of PA degradation and 6HPA accumulation. Filled symbols, PA degradation by KT2440 (▲) and KT/pBBR-*picA1A2A3* (■); open symbols, product 6HPA by KT2440 (△) and KT/pBBR-*picA1A2A3* (□). (B) HPLC profiles of PA degradation and 6HPA accumulation by the KT/pBBR-*picA1A2A3* strain. The detection wavelength was set at 280 nm. (C) LC/TOF-MS profile of the transformation product 6HPA. AU, arbitrary units.

to 3,6DHPA (23). BLAST homology searches against the NCBI database showed that *picB1*, *picB2*, *picB3*, and *picB4* had high levels of identity (35% to 45%) at the amino acid level with the respective components of four-component Rieske non-heme iron aromatic ring-hydroxylating oxygenases (RHOs) (Table 1; Fig. 4). RHOs are usually involved in the hydroxylation of aromatic compounds (32–34). Therefore, the genes *picB1B2B3B4* were predicted to encode a four-component RHO catalyzing the 3-hydroxylation of 6HPA to 3,6DHPA. The *picB1B2B3B4* genes were deleted from the genome of *A. faecalis* JQ135, and the resulting mutant JQ135 Δ*picB1B2B3B4* lost the ability to grow on PA or 6HPA but could still grow on 3,6DHPA (Fig. S4). The complemented strain JQ135 Δ*picB1B2B3B4*/pBBR-*picB1B2B3B4* regained the ability to grown on PA and 6HPA. The *picB1B2B3B4* genes were cloned into pBBR1MCS-5 and transferred into *P. putida*

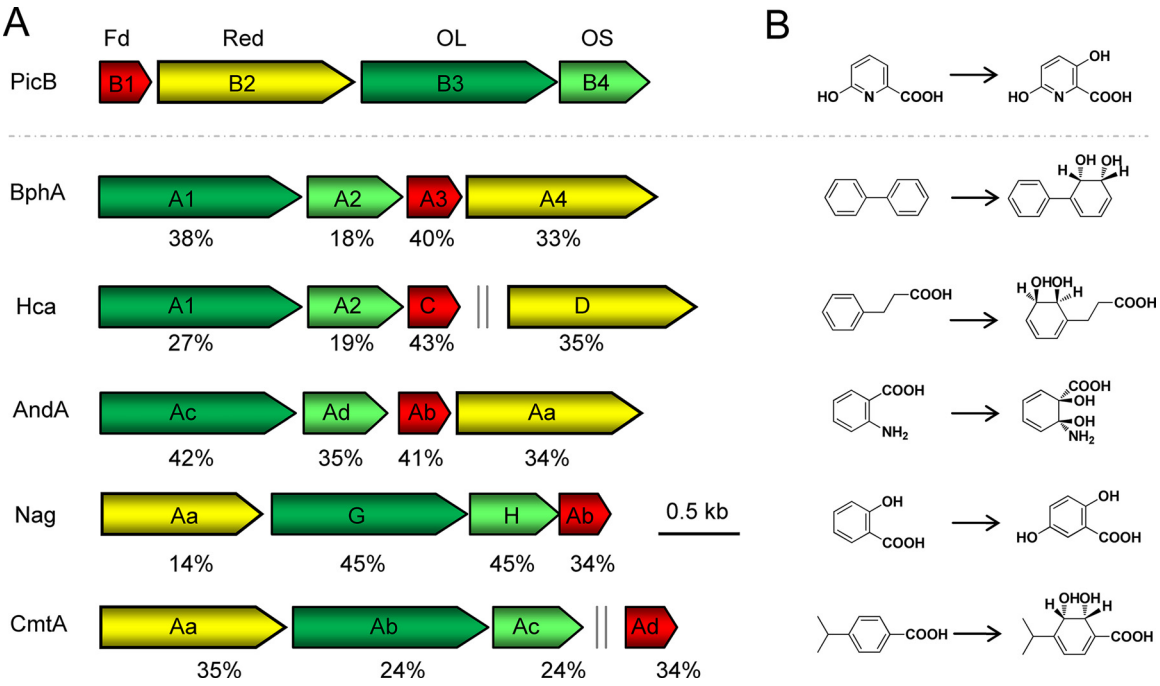

FIG 4 Genetic organizations of the PicB-encoding genes compared with similar Rieske non-heme iron aromatic ring-hydroxylating oxygenase genes (A) and the corresponding enzyme reactions (B). The arrows in panel A indicate the size and direction of each gene. Homologous genes are shown in the same color. Fd, ferredoxin; Red, reductase; OL, oxygenase large component; OS, oxygenase small component. Double vertical gray lines indicate discontinuous genes. Numbers below the arrows indicate the percent amino acid sequence identity with the ortholog *picB* gene product. BphA1A2A3A4 (GenBank accession numbers Q53122, Q53123, Q53124, and Q0S032), biphenyl 2,3-dioxygenase from *Rhodococcus jostii*; HcaA1A2CD (P0ABR5, Q47140, P0ABW0, and P77650), 3-phenylpropionate dioxygenase from *E. coli*; AndAaAbAcAd (Q84BZ0, Q84BZ1, Q84BZ3, and Q84BZ2), anthranilate 1,2-dioxygenase from *Burkholderia cepacia*; NagAaGHAb (O52378, O52379, O52380, and O52381), salicylate 5-hydroxylase from *Ralstonia* sp.; CmtAaAbAcAd (Q51973, Q51974, Q51975, and Q51978), *p*-cumate 2,3-dioxygenase from *Pseudomonas putida*.

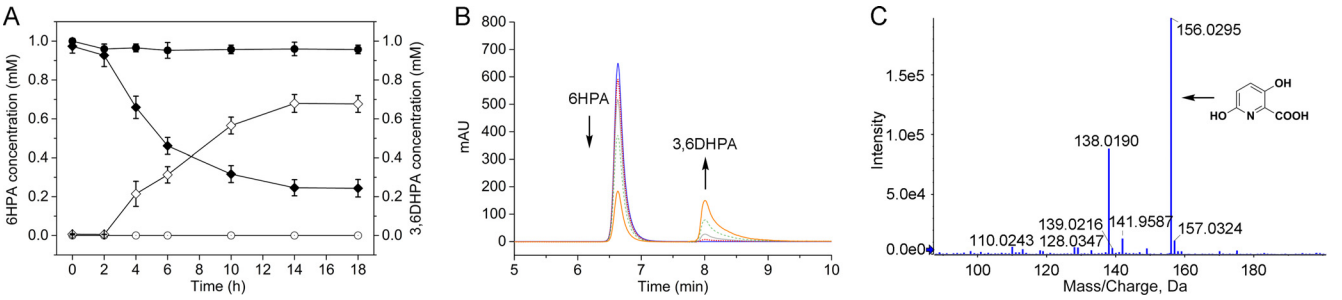

FIG 5 Conversion of 6HPA into 3,6DHPA by recombinant strain KT/pBBR-*picB1B2B3B4*. (A) The time course of 6HPA degradation and 3,6DHPA accumulation. Filled symbols, 6HPA degradation by KT2440 (●) and KT/pBBR-*picB1B2B3B4* (◆); open symbols, transformation product 3,6DHPA by KT2440 (○) and KT/pBBR-*picB1B2B3B4* (◇). (B) HPLC profiles of 6HPA degradation and 3,6DHPA accumulation by the KT/pBBR-*picB1B2B3B4* strain. The detection wavelength was set at 310 nm. (C) LC/TOF-MS profile of the transformation product 3,6DHPA.

KT2440. HPLC analysis showed that the recombinant KT/pBBR-*picB1B2B3B4* strain could degrade 6HPA with the appearance of one new peak in the HPLC chromatogram (Fig. 5). LC/TOF-MS analysis showed that this peak corresponded to 3,6DHPA [with a molecular ion peak ($[M+H]^+$) at 156.0295]. After degradation for 24 h, 0.75 mM 6HPA was depleted, and an approximately equal molar concentration of 3,6DHPA accumulated. Moreover, the recombinants KT/pBBR-*picB2B3B4* and KT/pBBR-*picB1B2B3* could not convert 6HPA (data not shown), suggesting that all four of these components were essential. These results indicated that the *picB1B2B3B4* genes encode a four-component RHO-type monooxygenase responsible for the conversion of 6HPA into 3,6DHPA in *A. faecalis* JQ135.

Interestingly, cell lysates of KT/pBBR-*picB1B2B3B4* grown in the presence of 6HPA were unable to convert 6HPA even though several cofactors (e.g., FAD, flavin mononucleotide [FMN], NADH, or NADPH) were added. Previous studies have attempted to purify the 6HPA monooxygenase from cell lysates of *Arthrobacter picolinophilus* DSM 20665 and the UGN strain; however, these studies were also unable to detect the PicB activity (23, 35). These results suggested that the PicB was unstable and readily lost activity.

PicDEF and PicG (MaiA) convert 2,5DHP into fumaric acid. Our previous study demonstrated that 3,6DHPA was converted to 2,5DHP by PicC in *A. faecalis* JQ135 (28). 2,5DHP is a central intermediate of many pyridine derivatives, including nicotinate (30), nicotine (36), 2-hydroxy-pyridine (24), and 5-hydroxypicolinic acid (26). Bacterial catabolism of 2,5DHP has been previously studied, and two 2,5DHP catabolic pathways have been reported: the hydroxylation and maleamate pathways. In the hydroxylation pathway, 2,5DHP is hydroxylated to 2,3,6-trihydroxypyridine, which spontaneously converts to a blue pigment (25). In the maleamate pathway, however, 2,5DHP is cleaved to *N*-formylmaleamic acid (NFM) by a dioxygenase, and NFM is then converted by a deformylase to maleamic acid, which is further deaminated by an amidohydrolase to maleic acid (24, 25, 30, 36, 37). Previous studies have shown that the four enzymes involved in this pathway are highly conserved (Fig. S5). In the *pic* gene cluster, three genes, *picD*, *picE*, and *picF*, are located downstream of *picC* (Fig. 1). PicD, PicE, and PicF show high similarities (40 to 60%) to 2,5DHP 5,6-dioxygenase, NFM deformylase, and maleamic acid amidohydrolase, respectively (Table 1; Fig. S5). This strongly implies that 2,5DHP is degraded via the maleamate pathway in *A. faecalis* JQ135. We overexpressed PicD in *Escherichia coli* BL21(DE3), and SDS-PAGE analysis showed an intense band at the predicted size of 6×His-tagged PicD (38 kDa) (Fig. S6). Purified PicD was able to convert 2,5DHP (Fig. S6), as measured spectrophotometrically by a decrease in absorbance at 320 nm (36, 37). No blue pigment accumulated in the enzymatic reaction, further suggesting that 2,5DHP was degraded via the maleamate pathway and not the hydroxylation pathway. Unfortunately, the expected product (NFM) was not detected, which might be due to the instability of NFM. PicD had a K_m value of 65.72 ± 6.27 μM and showed no activity without the addition of Fe^{2+} (Fig. S6), which resembles

previous reports of other 2,5DHP dioxygenases (30, 36, 37). To further investigate the function of the *picEDF* genes, a DNA fragment containing *picEDF* was cloned into *Sphingomonas wittichii* DC-6, which cannot degrade 2,5DHP (Fig. S7) (38). Recombinant DC-6/pBBR-*picEDF* acquired the ability to convert 2,5DHP to maleic acid (Fig. S8); however, the recombinant strain could not utilize 2,5DHP as a carbon source for growth (Fig. S7), which might be due to its inability to further degrade maleic acid to fumaric acid. These results further confirmed that the *picEDF* genes were responsible for conversion of 2,5DHP to maleic acid.

Maleic acid can be isomerized into fumaric acid, an intermediate of the Krebs cycle. However, the *pic* cluster lacks an isomerase-encoding gene. Bioinformatic analysis revealed that the gene *AFA_16520* (*maiA*, also named *picG* in this study) in the genome of *A. faecalis* JQ135, which is physically separated from the *pic* cluster, shares 99% similarity at the amino acid level with a maleic acid *cis-trans* isomerase MaiA from *A. faecalis* IFO13111 (39). Our previous study showed that PicG was essential for the utilization of PA, nicotinic acid, and 5-hydroxypicolinic acid (26). To further investigate the function of *picG*, this gene was deleted from *A. faecalis* JQ135, resulting in the mutant JQ135 Δ*picG*. The mutant strain could still degrade 2,5DHP but lost the ability to utilize the substrate for growth and accumulated maleic acid in the culture (Fig. S8). This result indicated that PicG was responsible for the isomerization of maleic acid to fumaric acid. Furthermore, a DNA fragment containing the *picEDFG* genes was cloned into *Sphingomonas wittichii* DC-6. Recombinant DC-6/pBBR-*picEDFG* acquired the ability to utilize 2,5DHP for growth (Fig. S7). These results confirmed that PicDEF and PicG (MaiA) are responsible for the conversion of 2,5DHP to fumaric acid.

Diversity of *pic* genes in other bacteria. Six complete genome sequences of *A. faecalis* strains (ZD02, P156, DSM 30030, J481, FDAARGOS_491, and BDB4) are available in NCBI, and *pic* gene clusters were identified in all of these genomes (Fig. 6; Table S1). Orthologous *pic* gene clusters were also found in other *Alpha-*, *Beta-*, and *Gammaproteobacteria* (21 genera and over 160 strains) (Table S1). Most of these strains belong to the order *Burkholderiales* of the class *Betaproteobacteria*, including the following genera: *Achromobacter*, *Alcaligenes*, *Advenella*, *Bordetella*, *Burkholderia*, *Caballeronia*, *Cupriavidus*, *Pandoraea*, *Paraburkholderia*, *Polaromonas*, *Pseudacidovorax*, *Pusillimonas*, *Ralstonia*, and *Variovorax*. Interestingly, some of these strains are toxic-compound degraders (e.g., *Achromobacter xylosoxidans* A8 and *Variovorax* sp. strain JS1663 (40, 41), human pathogens (e.g., *Bordetella pertussis* Tohama I and *Bordetella bronchiseptica* RB50) (42), and nematicidal bacteria (e.g., *A. faecalis* ZD02) (43), whereas other strains represent typical soil bacteria (e.g., *Pseudomonas*), plant rhizosphere-associated bacteria (e.g., *Bradyrhizobium*), arctic bacteria (*Octadecabacter arcticus* 238) (44), and Antarctic bacteria (*Hoeflea* sp. strain IMCC20628) (45).) Three of predicted degraders listed in Table S1 (*A. faecalis* ATCC 8750, *Cupriavidus pinatubonensis* JMP134 [46], and *Pusillimonas* sp. strain T2) were tested for their abilities to utilize PA. The results confirmed that these threes strains could utilize PA as a sole carbon source (Fig. S9). Previous reports also showed that bacteria in the *Aerococcus*, *Arthrobacter*, and *Streptomyces* genera could degrade PA (20, 22, 29). However, no orthologues of the *A. faecalis pic* genes were found in these bacteria, suggesting that other new and unknown catabolic genes may exist.

The genetic organization of the *pic* gene clusters in these bacteria was highly diverse (Fig. 6). The *picA* genes usually adjoin *picB* genes, except in *Cupriavidus* strains. In most genera, *picG* was located between *picC* and *picE*. However, in *Alcaligenes*, *Pusillimonas*, and some *Achromobacter* strains, *picG* was located at a site distant from the *pic* gene cluster. In *βeta-* and *Gammaproteobacteria*, PicB consists of four components. Interestingly, in *Alphaproteobacteria*, including the *Bradyrhizobium*, *Hoeflea*, and *Octadecabacter* genera, PicB consists of two components in which the large subunit PicB123 appears to be a fusion of PicB1, PicB2, and PicB3 (Fig. S10).

Conclusions. PA is generated through cell metabolism or synthesized artificially in industry and is thus ubiquitous in the environment. The degradation and detoxification of PA by microorganisms have been studied for more than 50 years (29). This study

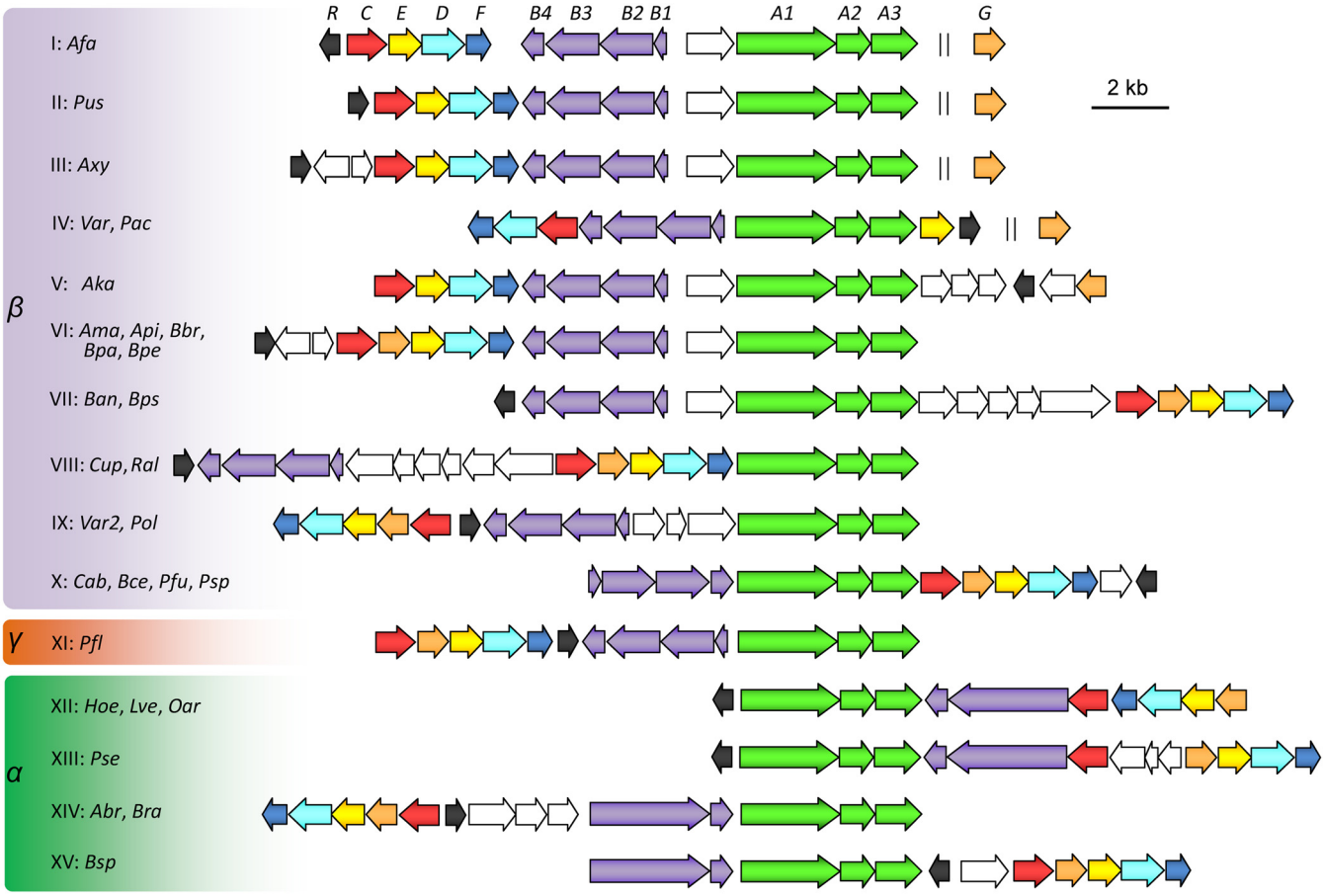

FIG 6 Predicted PA catabolism gene clusters in bacterial genomes. α, β, and γ indicate the *Alpha-*, *Beta-*, and *Gammaproteobacteria*. I to XV, the 15 different types of PA catabolism loci. Abbreviations and representative strains are as follows: *Afa*, *Alcaligenes faecalis* JQ135; *Pus*, *Pusillimonas* sp. strain T2; *Axy*, *Achromobacter xylosoxidans* A8; *Var*, *Variovorax paradoxus* S110; *Pac*, *Pseudacidovorax* sp. strain RU35E; *Aka*, *Advenella kashmirensis* W13003; *Ama*, *Achromobacter marplatensis* B2; *Api*, *Achromobacter piechaudii* ATCC 43553; *Bbr*, *Bordetella bronchiseptica* RB50; *Bpa*, *Bordetella parapertussis* ATCC BAA-587; *Bpe*, *Bordetella pertussis* Tohama I; *Ban*, *Bordetella ansorpii* NCTC13364; *Bps*, *Bordetella pseudohinzii* HI4681; *Cup*, *Cupriavidus necator* N-1; *Ral*, *Ralstonia pickettii* DTP0602; *Var2*, *Variovorax* sp. JS1663; *Pol*, *Polaromonas* sp. strain OV174; *Cab*, *Caballeronia arvi* LMG 29317; *Bce*, *Burkholderia cepacia* JBK9; *Pfu*, *Paraburkholderia fungorum* NBRC 102489; *Psp.*, *Pandoraea sputorum* DSM 21091; *Pfl*, *Pseudomonas fluorescens* C8; *Hoe*, *Hoeflea* sp. IMCC20628; *Lve*, *Loktanella vestfoldensis* SMR4r; *Oar*, *Octadecabacter arcticus* 238; *Pse*, *Paracoccus seriniphilus* DSM 14827; *Abr*, *Afipia broomeae* GAS525; *Bra*, *Bradyrhizobium canariense* GAS369; *Bsp.*, *Bradyrhizobium* sp. strain C9. The detailed genomic accession numbers and the gene locus tags are listed in Table S1 in the supplemental material. Identities (percent) of amino acid sequences between Pic proteins of strain *A. faecalis* JQ135 and representative homologs are listed in Table S2.

revealed that the *pic* gene cluster is responsible for the complete degradation of PA. PicA initially 6-hydroxylates PA to 6HPA, and then PicB 3-hydroxylates 6HPA to 3,6DHPA, which is then decarboxylated to 2,5DHP by PicC. 2,5DHP is further converted to fumaric acid via the maleamate pathway by the catalysis of PicD, PicE, PicF, and PicG. The genetic functions of *picA* and *picB* genes are reported here for the first time. In addition, the findings of homologous *pic* gene clusters in other *Alpha-*, *Beta-*, and *Gammaproteobacteria* help us understand the growth, competition, and environmental adaptability of bacteria in nature.

MATERIALS AND METHODS

Chemicals. PA, 6HPA, and 2,5DHP were purchased from J&K Scientific, Ltd. (Shanghai, China). 3,6DHPA was chemically synthesized (28), and other reagents were purchased from Sangon Biotech Co., Ltd. (Shanghai, China).

Strains, plasmids, and culture conditions. All bacterial strains and plasmids used in this study are listed in Table 2. Mineral salts medium (MSM) and Luria-Bertani (LB) medium have been previously described (26). *Alcaligenes faecalis* JQ135 is a wild-type PA-degrading strain (27). *Alcaligenes faecalis* ATCC 8750 was obtained from the China General Microbiological Culture Collection Center. *Cupriavidus pinatubonensis* JMP134 was a gift from Luying Xun (Shandong University) (46). *Pusillimonas* sp. strain T2 is a nicotinic acid-degrading bacterium (47). *P. putida* KT2440 is a model Gram-negative organism that cannot degrade or convert PA (30). *Sphingomonas wittichii* DC-6 is a chloroacetanilide herbicide degrader

TABLE 2 Strains and plasmids used in this study

Strain or plasmid	Description	Reference or source[a]
Alcaligenes faecalis strains		
ATCC 8750	Str^r; type strain	CGMCC 1.924
JQ135	Str^r; PA-degrading bacterium, Gram negative, wild type	CCTCC M 2015812
JQ135 Δ*picA1A2A3*	Str^r; *picA1A2A3* deletion mutant of JQ135	This study
JQ135 Δ*picA1A2A3*/pBBR-*picA1A2A3*	Str^r Gm^r; JQ135 Δ*picA1A2A3* complementation with pBBR-*picA1A2A3*	This study
JQ135 Δ*picB1B2B3B4*	Str^r; *picB1B2B3B4* deletion mutant of JQ135	This study
JQ135 Δ*picB1B2B3B4*/pBBR-*picB1B2B3B4*	Str^r Gm^r; JQ135 Δ*picB1B2B3B4* complementation with pBBR-*picB1B2B3B4*	This study
JQ135 Δ*picG*	Str^r; *maiA*(*AFA_16520*) deletion mutant of JQ135	26
Pseudomonas putida strains		
KT2440	Cm^r; metabolically versatile saprophytic soil strain, PA-nondegrading bacterium	ATCC 47054
KT/pBBR-*picA1A2A3*	Cm^r Gm^r; KT2440 containing plasmid pBBR-*picA1A2A3*	This study
KT/pBBR-*picA1A2*	Cm^r Gm^r; KT2440 containing plasmid pBBR-*picA1A2*	This study
KT/pBBR-*picA2A3*	Cm^r Gm^r; KT2440 containing plasmid pBBR-*picA2A3*	This study
KT/pBBR-*picB1B2B3B4*	Cm^r Gm^r; KT2440 containing plasmid pBBR-*picB1B2B3B4*	This study
KT/pBBR-*picB1B2B3*	Cm^r Gm^r; KT2440 containing plasmid pBBR-*picB1B2B3*	This study
KT/pBBR-*picB2B3B4*	Cm^r Gm^r; KT2440 containing plasmid pBBR-*picB2B3B4*	This study
Sphingomonas wittichii DC-6	Str^r; chloroacetanilide herbicide degrader, PA-nondegrading bacterium	KACC 16600
DC-6/pBBR-*picEDFG*	Str^r Gm^r; *S. wittichii* DC-6 containing pBBR-*picEDFG*	This study
DC-6/pBBR-*picEDF*	Str^r Gm^r; *S. wittichii* DC-6 containing pBBR-*picEDF*	This study
Pusillimonas sp. strain T2	Nicotinic acid-degrading bacterium	CCTCC M 2014272
Cupriavidus pinatubonensis JMP134	Hydrogen sulfide-oxidizing bacterium	46
E. coli strains		
DH5α	λ^- ϕ80d*lacZ*ΔM15 Δ(*lacZYA-argF*)*U169 recA1 endA hsdR17*(r_K^- m_K^-) *supE44 thi-1 gyrA relA1*	TaKaRa
BL21(DE3)	F^- *ompT* $hsdS_B$(r_B^- m_B^-) *gal dcm* (DE3)	TaKaRa
SM10 λpir	Donor strain for biparental mating	Lab stock
Plasmids		
pET29a(+)	Km^r; expression plasmid	Novagen
pJQ200SK	Gm^r Mob$^+$ *orip15A lacZα*$^+$ *sacB*; suicide plasmid	Lab stock
pBBR1MCS-5	Gm^r; broad-host-range cloning plasmid	Lab stock
pJQ-Δ*picA1A2A3*	Gm^r; *picA1A2A3* gene deletion plasmid; the upstream region of *picA1* gene and downstream region of *picA3* gene fused into SacI/PstI-digested pJQ200SK	This study
pJQ-Δ*picB1B2B3B4*	Gm^r; *picB1B2B3B4* gene deletion plasmid; the upstream region of *picB1* gene and downstream region of *picB4* gene fused into SacI/PstI-digested pJQ200SK	This study
pBBR-*picA1A2A3*	Gm^r; the fragment containing the *picA1A2A3* gene inserted into XhoI/HindIII-digested pBBR1MCS-5	This study
pBBR-*picA1A2*	Gm^r; the fragment containing the *picA1A2* gene inserted into XhoI/HindIII-digested pBBR1MCS-5	This study
pBBR-*picA2A3*	Gm^r; the fragment containing the *picA2A3* gene inserted into XhoI/HindIII-digested pBBR1MCS-5	This study
pBBR-*picB1B2B3B4*	Gm^r; the fragment containing the *picB1B2B3B4* gene inserted into XhoI/HindIII-digested pBBR1MCS-5	This study
pBBR-*picB1B2B3*	Gm^r; the fragment containing the *picB1B2B3* gene inserted into XhoI/HindIII-digested pBBR1MCS-5	This study
pBBR-*picB2B3B4*	Gm^r; the fragment containing the *picB2B3B4* gene inserted into XhoI/HindIII-digested pBBR1MCS-5	This study
pET-PicD	Km^r; *Nde*I-*Xho*I fragment containing *picD* gene inserted into pET29a(+)	This study

[a]CGMCC, China General Microbiological Culture Collection; CCTCC, China Center for Type Culture Collection; KACC, Korean Agricultural Culture Collection.

that is unable to degrade PA or 2,5DHP (38). *E. coli* DH5α acted as the host for the construction of plasmids. *E. coli* BL21(DE3) was used for protein overexpression. *E. coli* strains were grown in LB medium at 37°C. Antibiotics were added as required at the following concentrations: chloramphenicol (Cm), 34 mg/liter; gentamicin (Gm), 50 mg/liter; kanamycin (Km), 50 mg/liter; and streptomycin (Str), 50 mg/liter.

General DNA techniques. Routine isolation of genomic DNA, extraction of plasmids, restriction digestion, transformations, PCR, and electrophoresis were performed according to standard procedures described by Sambrook et al. (48). Primer synthesis and the sequencing of PCR products or plasmids were performed by Genscript Biotech (Nanjing, China). The primers used in this study are listed in Table 3.

TABLE 3 Primers used in this study

Primer	Sequence (5→3)	Description
kopicA1A2A3-UF	AGCTTGATATCGAATTCCTGCAGCTGATTTTGCCAAGATCTATC	To construct plasmid pJQ-Δ*picA1A2A3*
kopicA1A2A3-UR	TCTAGAACTAGTGGATCCTTCCATCGGCAACATGCACTGC	
kopicA1A2A3-DF	GGATCCACTAGTTCTAGACCGTCGTGGCCGAGTTCAATCC	
kopicA1A2A3-DR	AGGGAACAAAAGCTGGAGCTCGGCAGGCAACATGAACAGCAC	
kopicB1B2B3B4-UF	AGCTTGATATCGAATTCCTGCAGACTCGGAGCGCGACTGCTCAC	To construct plasmid pJQ-Δ*picB1B2B3B4*
kopicB1B2B3B4-UR	TCTAGAACTAGTGGATCCGTATAAGTCCGTGGTTTGCATC	
kopicB1B2B3B4-DF	GGATCCACTAGTTCTAGAGTTTCGGAAATTTTTATCCAGT	
kopicB1B2B3B4-DR	AGGGAACAAAAGCTGGAGCTCTCTGCGCGTAAGGCACCAGTTC	
picA1A2A3-F	CAGGAATTCGATATCAAGCTTTACGACAAGTCTCAGGAGCTGTGG	To construct plasmid pBBR-*picA1A2A3*
picA1A2A3-R	GGTACCGGGCCCCCCCTCGAGGTACCATTGCACTTCCAGCCAGG	
picA1A2-F	CAGGAATTCGATATCAAGCTTTACGACAAGTCTCAGGAGCTGTGG	To construct plasmid pBBR-*picA1A2*
picA1A2-R	GGTACCGGGCCCCCCCTCGAGGTCGCGGCTGGTGGCCAACATGC	
picA2A3-F	CAGGAATTCGATATCAAGCTTATCGCCCAATACGGAGTTTGG	To construct plasmid pBBR-*picA2A3*
picA2A3-R	GGTACCGGGCCCCCCCTCGAGGTACCATTGCACTTCCAGCCAGG	
picB1B2B3B4-F	GGTACCGGGCCCCCCCTCGAGGTTGCGGCCGTTGCCGATTTCAG	To construct plasmid pBBR-*picB1B2B3B4*
picB1B2B3B4-R	CAGGAATTCGATATCAAGCTTGGAATCAGAAGACCTTCTGACTC	
picB1B2B3-F	GGTACCGGGCCCCCCCTCGAGGTTGCGGCCGTTGCCGATTTCAG	To construct plasmid pBBR-*picB1B2B3*
picB1B2B3-R	CAGGAATTCGATATCAAGCTTACGATCCAACGTGGCACAGTAC	
picB2B3B4-F	GGTACCGGGCCCCCCCTCGAGGTAGAAACTGGCCCTGCACAAACTGG	To construct plasmid pBBR-*picB2B3B4*
picB2B3B4-R	CAGGAATTCGATATCAAGCTTGGAATCAGAAGACCTTCTGACTC	
picEDF-F	CAGGAATTCGATATCAAGCTTCATCGGCAGCAATATTCTGATCACC	To construct plasmid pBBR-*picEDF*
picEDF-R	GGTACCGGGCCCCCCCTCGAGGTCACATCGTTCTTCTCAAATAC	
picEDFG-F1	CAGGAATTCGATATCAAGCTTCATCGGCAGCAATATTCTGATCACC	To construct plasmid pBBR-*picEDFG*
picEDFG-R1	CCAAGCATCGTCGCACATTTCCCACATCGTTCTTCTCAAATAC	
picEDFG-F2	GGAAATGTGCGACGATGCTTGG	
picEDFG-R2	GGTACCGGGCCCCCCCTCGAGGTGGCAGGGCTGTGTACTGCTAAG	
expPicD-F	CTTTAAGAAGGAGATATACATATGAGCACATTTTTGTATGGC	To construct plasmid pET-PicD
expPicD-R	GTGGTGGTGGTGGTGGTGCTCGAGCACCAAGCGCTGGCCCAG	
RT-16S F	CGCGGTAATACGTAGGGTG	To amplify fragment 16S shown in Fig. 1
RT-16S R	AACTTCACGCGTTAGCTGCG	
RT-1 F	TCGTCGGGGTTGATACGACG	To amplify fragment 1 shown in Fig. 1
RT-1 R	GGCCGACATCCTGGGTCCAGTG	
RT-2 F	GTACGTCGTGCTGTCGCAGACT	To amplify fragment 2 shown in Fig. 1
RT-2 R	ATAGAACGGCACATCCAGCTT	
RT-3 F	GGCAGTAACTTGGGGTTTTGTGG	To amplify fragment 3 shown in Fig. 1
RT-3 R	AGAAGGCGCGCATATCCTCAG	
RT-4 F	AGATTGCCGCTCAGTCCATGG	To amplify fragment 4 shown in Fig. 1
RT-4 R	TCACGAATCGCAGGGAATTC	
RT-5 F	GCAACGGCACGTGAGCAG	To amplify fragment 5 shown in Fig. 1
RT-5 R	CAACCGCTGGTAACCGCAC	
RT-6 F	ATACCGGGAACACCAGATCGTTCG	To amplify fragment 6 in Fig. 1
RT-6 R	ATTGAGGCCGAGGGTAATTTCATGC	
RT-7 F	GCATACTTGTCCTCGGACTTGG	To amplify fragment 7 in Fig. 1
RT-7 R	ACCAGTGGTCTTACAGCCTGAAGG	
RT-8 F	ATCCTGCCCGACAATGGCG	To amplify fragment 8 in Fig. 1
RT-8 R	CACTGTCATTGAAGCGAATG	
RT-9 F	AGGCCTGGCTAAAGTCAGCC	To amplify fragment 9 in Fig. 1
RT-9 R	AAATTTCCGAAACCGATGC	
RT-10 F	CGCCGCCCGTGCTGACCGC	To amplify fragment 10 in Fig. 1
RT-10 R	GCAGGCGGCCTTCATTGC	
RT-11 F	CCCACGCTCAGATTGAAGA	To amplify fragment 11 in Fig. 1
RT-11 R	ACATCCACAGACTCAATAAAC	
RT-12 F	GAACGGCTTTACGACGTTTG	To amplify fragment 12 in Fig. 1
RT-12 R	TCCAACGTGGCATTGCCCTTGAAGG	
RT-13 F	CCGCATGAGCGTGATGGC	To amplify fragment 13 in Fig. 1
RT-13 R	TCGTGGTTCAGGCGCTTGAC	

Construction of recombinant plasmids and heterologous expression. Genes from *A. faecalis* JQ135 were PCR amplified using the corresponding primers (Table 3). Amplified DNA fragments were cloned into digested plasmids using a ClonExpress MultiS One Step Cloning kit (Vazyme Biotech Co., Ltd., Nanjing, China).

The plasmid pBBR1MCS-5 (49) was used for heterologous expression in *P. putida* KT2440. PCR products and XhoI/HindIII-digested plasmids were ligated, and the resulting recombinant plasmids were transferred into *P. putida* KT2440 by biparental mating using SM10 λpir.

To test the components of the PA dehydrogenase, pBBR1MCS-5-based plasmid clones containing different gene combinations (*picA1A2A3*, *picA1A2*, and *picA2A3*) were transferred into *P. putida* KT2440 to

yield the recombinants KT/pBBR-*picA1A2A3*, KT/pBBR-*picA1A2*, and KT/pBBR-*picA2A3*, respectively. Similarly, to test the components of the 6HPA monooxygenase, the strains KT/pBBR-*picB1B2B3B4*, KT/pBBR-*picB1B2B3*, and KT/pBBR-*picB2B3B4* were constructed.

For overexpression of the *picD* gene in *E. coli* BL21(DE3), the complete open reading frame (ORF) without its corresponding stop codon was amplified and inserted into NdeI/XhoI-digested plasmid pET29a(+), resulting in the plasmid pET-PicD. The induction and purification of 6×His-tagged PicD from *E. coli* BL21(DE3) (containing pET-PicD) were performed as previously described (26). Purified 6×His-tagged PicD was then analyzed by 12.5% SDS-PAGE. Protein concentration was determined using the Bradford method (50).

Gene knockout and genetic complementation of *A. faecalis* JQ135. Deletion mutants of the *picA1A2A3* and *picB1B2B3B4* genes in *A. faecalis* JQ135 were constructed using a two-step homologous recombination method with the suicide plasmid pJQ200SK (51). Using the deletion of *picA1A2A3* as an example, two homologous recombination-directing sequences (500 to 1,000 bp) were amplified using primers kopicA1A2A3-UF/-UR and kopicA1A2A3-DF/-DR, respectively. The two PCR fragments were subsequently ligated into SacI/PstI-digested pJQ200SK yielding pJQ-Δ*picA1A2A3*. The plasmid pJQ-Δ*picA1A2A3* was then introduced into *A. faecalis* JQ135 cells. Single-crossover mutants were screened on LB plates containing Str and Gm. Gentamicin-resistant colonies were then subjected to repeated cultivation in LB medium containing 10% sucrose and no gentamicin. Double-crossover mutants, which had lost their vector backbones and were sensitive to gentamicin, were selected on LB-Str plates. Deletion of the *picA1A2A3* genes was confirmed by PCR. This procedure resulted in construction of the deletion mutant strain JQ135 Δ*picA1A2A3*.

Knockout mutants were complemented with the corresponding gene(s). For example, the complete *picA1A2A3* genes were amplified with primers picA1A2A3-F/-R and then ligated with XhoI/HindIII-digested pBBR1-MCS5, generating pBBR-*picA1A2A3*. The pBBR-*picA1A2A3* vector was transferred into the mutant strain JQ135 Δ*picA1A2A3* to generate the complemented strain JQ135 Δ*picA1A2A3*/pBBR-*picA1A2A3*.

Preparation of resting cells and biodegradation assays. Resting cells were prepared as follows. *Alcaligenes*, *Pseudomonas*, and *Sphingomonas* strains and their derivates were grown in 250-ml Erlenmeyer flasks with 100 ml of LB medium at 30°C and 180 rpm. When late exponential phase was reached, the cells were harvested by centrifugation at 4°C and 6,000 rpm for 10 min. The cells were washed twice with MSM and finally resuspended in MSM. The optical density at 600 nm (OD_{600}) was adjusted to 2.0. These cells were named resting cells.

For the growth experiment, resting cells (such as JQ135 Δ*picA1A2A3*) were added to MSM with 1 mM substrate (PA, 6HPA, or 3,6DHPA) for preincubation. After 24 h, the precultured cells were recollected, washed with MSM, and resuspended in MSM at a final OD_{600} of 2.0. Precultured cells were used for inoculation of MSM with 1 mM substrate. The initial OD_{600} was set at 0.15 to 0.2.

For biotransformation experiments, resting cells (such as KT/pBBR-*picA1A2A3*) were added to MSM with 1 mM substrate (PA or 6HPA) and 1 mM citrate for preincubation. After 12 h, the precultured cells were recollected, washed with MSM, and resuspended in MSM. The initial OD_{600} was set as 2.0, and then 1 mM substrate was added.

The growth and biotransformation experiments were all conducted in triplicate in 50-ml Erlenmeyer flasks with 20 ml of MSM at 30°C and 180 rpm. Samples (0.5 ml per time point) were collected periodically from the cultures. The growth of cells was monitored by measuring the OD_{600}. The concentrations of substrate or products were measured by HPLC.

RT-PCR. *A. faecalis* JQ135 resting cells were inoculated into 50-ml flasks with 20 ml of MSM containing 1 mM PA or citrate and cultured at 30°C and 180 rpm. The initial OD_{600} of the cultures was adjusted to 0.5. After 8 h, 5 ml of the culture was harvested by centrifugation at 4°C and 12,000 rpm for 10 min. Total RNA was isolated using an RNA isolation kit (TaKaRa), and reverse transcription-PCR (RT-PCR) was carried out with a PrimeScript RT reagent kit (TaKaRa) according to the manufacturer's protocol. The cDNA was then used as a template in the following PCR amplification reaction mixtures: 10 μl of 2×SYBRPremix Ex Taq (TaKaRa), 0.8 μl of primers (10 μM), 2 μl of cDNA, and 7.2 μl of H_2O. The primers used for RT-PCR are listed in Table 3. All samples were run in triplicate.

Enzymatic assays. PA dehydrogenase (PicA) assays were performed using cell extracts of KT/pBBR-*picA1A2A3*. Resting KT/pBBR-*picA1A2A3* cells were added into MSM containing 1 mM citrate and 1 mM PA. Following incubation for 12 h, cells were harvested by centrifugation at 6,000 rpm for 10 min at 4°C. Cell pellets were then resuspended in 50 mM phosphate buffered saline (PBS) (pH 7.0) and disrupted by sonication in an ice water bath. Cell-free extracts were obtained by centrifugation of cell lysates at 16,000 × *g* for 30 min at 4°C. The supernatant was used for PA dehydrogenase assays, while PicA activity was analyzed spectrophotometrically at 25°C by the formation of 6HPA at 310 nm ($\varepsilon = 4.45\ cm^{-1}\ mM^{-1}$) using a UV2450 spectrophotometer (Shimadzu) in 1-cm-path-length quartz cuvettes (23). The 1-ml reaction mixture contained 50 mM PBS (pH 7.0), 1 to 10 μg of total protein from the cell extract, 1 mM PA, and 1 mM electron acceptor PMS, and the reaction was started by adding PA. One unit of activity was defined as the amount of enzyme that catalyzed the formation of 1 μmol of 6HPA in 1 min.

For the 6HPA monooxygenase (PicB) assays, cell extracts of KT/pBBR-*picB1B2B3B4* were used. The preparation of cell extracts was the same as that for KT/pBBR-*picA1A2A3*. PicB activity was analyzed spectrophotometrically by observing the formation of 3,6DHPA at 360 nm ($\varepsilon = 4.4\ cm^{-1}\ mM^{-1}$) (28). The 1-ml reaction mixture contained 50 mM PBS (pH 7.0), 1 to 10 μg of total protein from cell extract, 1 mM 6HPA, and 1 mM electron donor (NADH, NADPH, FAD, or FMN), and the reaction was started by the addition of 6HPA. One unit of activity was defined as the amount of enzyme that catalyzed the formation of 1 μmol of 3,6DHPA in 1 min.

The 2,5DHP dioxygenase (PicD) assays were performed similarly to those previously performed for NicX from *P. putida* KT2440 (30) and VppE in *Ochrobactrum* sp. strain SJY1 (36). A 1-ml reaction mixture containing 50 mM PBS (pH 7.0), 0.2 mM 2,5DHP, 0.1 μg of purified PicD, and 1 mM Fe^{2+} was incubated at 25°C. Activity was assayed spectrophotometrically by measuring the reduction in absorbance at 320 nm ($\varepsilon = 5.2\ cm^{-1}\ mM^{-1}$), which corresponded to the disappearance of 2,5DHP (30, 36, 37). One unit of activity was defined as the amount of enzyme that catalyzed the consumption of 1 μmol of 2,5DHP in 1 min.

Analytical methods. The determination of PA and 6HPA, 3,6DHPA, 2,5DHP, and maleic acid was performed by UV-visible spectroscopy, HPLC, and LC/TOF-MS analysis as described previously (28).

Data availability. The *pic* gene cluster sequence and the complete genome sequence of *Alcaligenes faecalis* JQ135 have been deposited in the GenBank/DDBJ/EMBL database under the accession numbers KY264362 and CP021641, respectively.

Comparisons of the Pic proteins were performed against the nonredundant protein (nr) sequence database using BLASTP (protein-protein BLAST) on the NCBI website, employing an expect (E) value inclusion threshold of 10. Conserved protein domains were analyzed using the Conserved Domain Database (CDD [https://www.ncbi.nlm.nih.gov/Structure/cdd/wrpsb.cgi]). The genome sequence accession numbers of other strains and the corresponding locus tags of the *pic* gene clusters are listed in Table S1 in the supplemental material.

SUPPLEMENTAL MATERIAL

Supplemental material for this article may be found at https://doi.org/10.1128/JB.00077-19.

SUPPLEMENTAL FILE 1, PDF file, 1.8 MB.

SUPPLEMENTAL FILE 2, XLSX file, 0.04 MB.

SUPPLEMENTAL FILE 3, XLSX file, 0.01 MB.

ACKNOWLEDGMENTS

We are grateful to Luying Xun (Shandong University) for his kind provision of strain *Cupriavidus pinatubonensis* JMP134.

This work was supported by the National Science and Technology Major Project (2018ZX0800907B-002), the National Natural Science Foundation of China (grants 41630637, 31870092, 31770117, and 31600080), and the Key R&D Program Project in Jiangsu Province (BE2016374).

We declare that we have no conflicts of interest.

REFERENCES

1. Heyes MP, Chen CY, Major EO, Saito K. 1997. Different kynurenine pathway enzymes limit quinolinic acid formation by various human cell types. Biochem J 326:351–356. https://doi.org/10.1042/bj3260351.
2. Bryleva EY, Brundin L. 2017. Kynurenine pathway metabolites and suicidality. Neuropharmacology 112:324–330. https://doi.org/10.1016/j.neuropharm.2016.01.034.
3. Esquivel DG, Ramirez-Ortega D, Pineda B, Castro N, Rios C, de la Cruz VP. 2017. Kynurenine pathway metabolites and enzymes involved in redox reactions. Neuropharmacology 112:331–345. https://doi.org/10.1016/j.neuropharm.2016.03.013.
4. Nishino SF, Spain JC. 1993. Degradation of nitrobenzene by a *Pseudomonas pseudoalcaligenes*. Appl Environ Microbiol 59:2520–2525.
5. Mehler AH. 1956. Formation of picolinic and quinolinic acids following enzymatic oxidation of 3-hydroxyanthranilic acid. J Biol Chem 218:241–254.
6. Asano Y, Yamamoto Y, Yamada H. 1994. Catechol 2,3-dioxygenase-catalyzed synthesis of picolinic acids from catechols. Biosci Biotechnol Biochem 58:2054–2056. https://doi.org/10.1271/bbb.58.2054.
7. Chirino B, Strahsburger E, Agullo L, Gonzalez M, Seeger M. 2013. Genomic and functional analyses of the 2-aminophenol catabolic pathway and partial conversion of its substrate into picolinic acid in *Burkholderia xenovorans* LB400. PLoS One 8:e75746. https://doi.org/10.1371/journal.pone.0075746.
8. Abdullaev M, Klyuev M, Abdullaeva ZS, Kurbanov B, Idrisova A. 2008. Preparation of lidocaine, bipuvacaine, mepivacaine, trimecaine, and pyromecaine by reductive acylation on palladium catalysts. Pharm Chem J 42:357–359. https://doi.org/10.1007/s11094-008-0126-6.
9. McCall PJ, Agin GL. 1985. Desorption kinetics of picloram as affected by residence time in the soil. Environ Toxicol Chem 4:37–44. https://doi.org/10.1002/etc.5620040106.
10. Broadhurst CL, Domenico P. 2006. Clinical studies on chromium picolinate supplementation in diabetes mellitus—a review. Diabetes Technol Ther 8:677–687. https://doi.org/10.1089/dia.2006.8.677.
11. Martin J, Wang ZQ, Zhang XH, Wachtel D, Volaufova J, Matthews DE, Cefalu WT. 2006. Chromium picolinate supplementation attenuates body weight gain and increases insulin sensitivity in subjects with type 2 diabetes. Diabetes Care 29:1826–1832. https://doi.org/10.2337/dc06-0254.
12. Ogata S, Inoue K, Iwata K, Okumura K, Taguchi H. 2001. Apoptosis induced by picolinic acid-related compounds in HL-60 cells. Biosci Biotechnol Biochem 65:2337–2339. https://doi.org/10.1271/bbb.65.2337.
13. Cioczek-Czuczwar A, Czuczwar P, Turski WA, Parada-Turska J. 2017. Influence of picolinic acid on seizure susceptibility in mice. Pharmacol Rep 69:77–80. https://doi.org/10.1016/j.pharep.2016.10.009.
14. Prodinger J, Loacker LJ, Schmidt RL, Ratzinger F, Greiner G, Witzeneder N, Hoermann G, Jutz S, Pickl WF, Steinberger P. 2015. The tryptophan metabolite picolinic acid suppresses proliferation and metabolic activity of $CD4^+$ T cells and inhibits c-Myc activation. J Leukoc Biol 99:583–594. https://doi.org/10.1189/jlb.3A0315-135R.
15. Nakata HM, Halvorson HO. 1960. Biochemical changes occurring during growth and sporulation of *Bacillus cereus*. J Bacteriol 80:801–810.
16. Tamer Ö, Tamer SA, İdil Ö, Avcı D, Vural H, Atalay Y. 2018. Antimicrobial activities, DNA interactions, spectroscopic (FT-IR and UV-Vis) characterizations, and DFT calculations for pyridine-2-carboxylic acid and its derivates. J Mol Struct 1152:399–408. https://doi.org/10.1016/j.molstruc.2017.09.100.
17. Suksrichavalit T, Prachayasittikul S, Nantasenamat C, Isarankura-Na-Ayudhya C, Prachayasittikul V. 2009. Copper complexes of pyridine derivatives with superoxide scavenging and antimicrobial activities. Eur J Med Chem 44:3259–3265. https://doi.org/10.1016/j.ejmech.2009.03.033.
18. Smythe GA, Poljak A, Bustamante S, Braga O, Maxwell A, Grant R,

Sachdev P. 2003. ECNI GC-MS analysis of picolinic and quinolinic acids and their amides in human plasma, CSF, and brain tissue, p 705–712. *In* Allegri G, Cost CVL, Ragazzi E, Steinhart H, Varesio L (ed), Developments in tryptophan and serotonin metabolism. Springer, New York, NY.
19. Kiener A, Glockler R, Heinzmann K. 1993. Preparation of 6-oxo-1,6-dihydropyridine-2-carboxylic acid by microbial hydroxylation of pyridine-2-carboxylic acid. J Chem Soc Perkin 1:1201–1202. https://doi.org/10.1039/P19930001201.
20. Siegmund I, Koenig K, Andreesen JR. 1990. Molybdenum involvement in aerobic degradation of picolinic acid by *Arthrobacter picolinophilus*. FEMS Microbiol Lett 67:281–284. https://doi.org/10.1016/0378-1097(90)90009-F.
21. Zheng C, Wang Q, Ning Y, Fan Y, Feng S, He C, Zhang TC, Shen Z. 2017. Isolation of a 2-picolinic acid-assimilating bacterium and its proposed degradation pathway. Bioresource Technol 245:681–688. https://doi.org/10.1016/j.biortech.2017.09.031.
22. Zheng C, Zhou J, Wang J, Qu B, Wang J, Lu H, Zhao H. 2009. Aerobic degradation of 2-picolinic acid by a nitrobenzene-assimilating strain: *Streptomyces* sp. Z2. Bioresource Technol 100:2082–2084. https://doi.org/10.1016/j.biortech.2008.10.017.
23. Orpin CG, Knight M, Evans WC. 1972. The bacterial oxidation of picolinamide, a photolytic product of Diquat. Biochem J 127:819–831. https://doi.org/10.1042/bj1270819.
24. Petkevičius V, Vaitekūnas J, Stankevičiūtė J, Gasparavičiūtė R, Meškys R. 2018. Catabolism of 2-hydroxypyridine by *Burkholderia* sp. strain MAK1: a 2-hydroxypyridine 5-monooxygenase encoded by *hpdABCDE* catalyzes the first step of biodegradation. Appl Environ Microbiol 84:e00387-18.
25. Kaiser JP, Feng YC, Bollag JM. 1996. Microbial metabolism of pyridine, quinoline, acridine, and their derivatives under aerobic and anaerobic conditions. Microbiol Rev 60:483–498.
26. Qiu J, Liu B, Zhao L, Zhang Y, Cheng D, Yan X, Jiang J, Hong Q, He J. 2018. A novel degradation mechanism for pyridine derivatives in *Alcaligenes faecalis* JQ135. Appl Environ Microbiol 84:e00910-18. https://doi.org/10.1128/AEM.00910-18.
27. Qiu J, Zhang J, Zhang Y, Wang Y, Tong L, Hong Q, He J. 2017. Biodegradation of picolinic acid by a newly isolated bacterium *Alcaligenes faecalis* strain JQ135. Curr Microbiol 74:508–514. https://doi.org/10.1007/s00284-017-1205-2.
28. Qiu J, Zhang Y, Yao S, Ren H, Qian M, Hong Q, Lu Z, He J. 2019. Novel 3, 6-dihydroxypicolinic acid decarboxylase mediated picolinic acid catabolism in *Alcaligenes faecalis* JQ135. J Bacteriol 201:e00665-18. https://doi.org/10.1128/JB.00665-18.
29. Dagley S, Johnson PA. 1963. Microbial oxidation of kynurenic, xanthurenic and picolinic acids. Biochim Biophys Acta 78:577–587. https://doi.org/10.1016/0006-3002(63)91023-0.
30. Jiménez JI, Canales A, Jiménez-Barbero J, Ginalski K, Rychlewski L, García JL, Díaz E. 2008. Deciphering the genetic determinants for aerobic nicotinic acid degradation: the *nic* cluster from *Pseudomonas putida* KT2440. Proc Natl Acad Sci U S A 105:11329–11334. https://doi.org/10.1073/pnas.0802273105.
31. Grether-Beck S, Igloi GL, Pust S, Schilz E, Decker K, Brandsch R. 1994. Structural analysis and molybdenum-dependent expression of the pAO1-encoded nicotine dehydrogenase genes of *Arthrobacter nicotinovorans*. Mol Microbiol 13:929–936. https://doi.org/10.1111/j.1365-2958.1994.tb00484.x.
32. Chakraborty J, Ghosal D, Dutta A, Dutta TK. 2012. An insight into the origin and functional evolution of bacterial aromatic ring-hydroxylating oxygenases. J Biomol Struct Dyn 30:419–436. https://doi.org/10.1080/07391102.2012.682208.
33. Vaitekūnas J, Gasparavičiūtė R, Rutkienė R, Tauraitė D, Meškys R. 2016. A 2-hydroxypyridine catabolism pathway in *Rhodococcus rhodochrous* strain PY11. Appl Environ Microbiol 82:1264. https://doi.org/10.1128/AEM.02975-15.
34. Li A, Qu Y, Zhou J, Ma F. 2009. Enzyme-substrate interaction and characterization of a 2,3-dihydroxybiphenyl 1, 2-dioxygenase from *Dyella ginsengisoli* LA-4. FEMS Microbiol Lett 292:231–239. https://doi.org/10.1111/j.1574-6968.2009.01487.x.
35. Tate R, Ensign J. 1974. Picolinic acid hydroxylase of *Arthrobacter picolinophilus*. Can J Microbiol 20:695–702. https://doi.org/10.1139/m74-106.
36. Yu H, Tang H, Zhu X, Li Y, Xu P. 2015. Molecular mechanism of nicotine degradation by a newly isolated strain, *Ochrobactrum* sp. strain SJY1. Appl Environ Microbiol 81:272–281. https://doi.org/10.1128/AEM.02265-14.
37. Tang H, Yao Y, Wang L, Yu H, Ren Y, Wu G, Xu P. 2012. Genomic analysis of *Pseudomonas putida*: genes in a genome island are crucial for nicotine degradation. Sci Rep 2:377. https://doi.org/10.1038/srep00377.
38. Chen Q, Wang C-H, Deng S-K, Wu Y-D, Li Y, Yao L, Jiang J-D, Yan X, He J, Li S-P. 2014. Novel three-component Rieske non-heme iron oxygenase system catalyzing the *N*-dealkylation of chloroacetanilide herbicides in sphingomonads DC-6 and DC-2. Appl Environ Microbiol 80:5078–5085. https://doi.org/10.1128/AEM.00659-14.
39. Hatakeyama K, Asai Y, Uchida Y, Kobayashi M, Terasawa M, Yukawa H. 1997. Gene cloning and characterization of maleate *cis-trans* isomerase from *Alcaligenes faecalis*. Biochem Biophys Res Commun 239:74–79. https://doi.org/10.1006/bbrc.1997.7430.
40. Strnad H, Ridl J, Paces J, Kolar M, Vlcek C, Paces V. 2011. Complete genome sequence of the haloaromatic acid-degrading bacterium *Achromobacter xylosoxidans* A8. J Bacteriol 193:791–792. https://doi.org/10.1128/JB.01299-10.
41. Mahan KM, Zheng H, Fida TT, Parry RJ, Graham DE, Spain JC. 2017. Iron-dependent enzyme catalyzes the initial step in biodegradation of *N*-nitroglycine by *Variovorax* sp. strain JS1663. Appl Environ Microbiol 83:e00457-17. https://doi.org/10.1128/AEM.00457-17.
42. Parkhill J, Sebaihia M, Preston A, Murphy LD, Thomson N, Harris DE, Holden MTG, Churcher CM, Bentley SD, Mungall KL, Cerdeño-Tárraga AM, Temple L, James K, Harris B, Quail MA, Achtman M, Atkin R, Baker S, Basham D, Bason N, Cherevach I, Chillingworth T, Collins M, Cronin A, Davis P, Doggett J, Feltwell T, Goble A, Hamlin N, Hauser H, Holroyd S, Jagels K, Leather S, Moule S, Norberczak H, O'Neil S, Ormond D, Price C, Rabbinowitsch E, Rutter S, Sanders M, Saunders D, Seeger K, Sharp S, Simmonds M, Skelton J, Squares R, Squares S, Stevens K, Unwin L, Whitehead S, Barrell BG, Maskell DJ. 2003. Comparative analysis of the genome sequences of *Bordetella pertussis*, *Bordetella parapertussis* and *Bordetella bronchiseptica*. Nat Genet 35:32. https://doi.org/10.1038/ng1227.
43. Ju S, Lin J, Zheng J, Wang S, Zhou H, Sun M. 2016. *Alcaligenes faecalis* ZD02, a novel nematicidal bacterium with an extracellular serine protease virulence factor. Appl Environ Microbiol 82:2112–2120. https://doi.org/10.1128/AEM.03444-15.
44. Vollmers J, Voget S, Dietrich S, Gollnow K, Smits M, Meyer K, Brinkhoff T, Simon M, Daniel R. 2013. Poles apart: Arctic and Antarctic *Octadecabacter* strains share high genome plasticity and a new type of xanthorhodopsin. PLoS One 8:e63422. https://doi.org/10.1371/journal.pone.0063422.
45. Cubillas C, Miranda-Sánchez F, González-Sánchez A, Elizalde JP, Vinuesa P, Brom S, García-De L. 2017. A comprehensive phylogenetic analysis of copper transporting P_{1B} ATPases from bacteria of the *Rhizobiales* order uncovers multiplicity, diversity and novel taxonomic subtypes. Microbiologyopen 6:e452. https://doi.org/10.1002/mbo3.452.
46. Li H, Li J, Lü C, Xia Y, Xin Y, Liu H, Xun L, Liu H. 2017. FisR activates σ^{54}-dependent transcription of sulfide-oxidizing genes in *Cupriavidus pinatubonensis* JMP 134. Mol Microbiol 105:373–384. https://doi.org/10.1111/mmi.13725.
47. Yuan M, Zhang Y, Zhao L, Ma Y, He Q, He J, Qiu J. 2018. Identification and characterization of a new three-component nicotinic acid hydroxylase NahAB1B2 from *Pusillimonas* sp. strain T2. Lett Appl Microbiol 66:321–328. https://doi.org/10.1111/lam.12850.
48. Sambrook J, Russell DW. 2001. Molecular cloning: a laboratory manual, 3rd ed. Cold Spring Harbor Laboratory Press, Cold Spring Harbor, NY.
49. Kovach M, Elzer P, Hill D, Robertson G, Farris M, Roop R, Peterson K. 1995. Four new derivatives of the broad-hostrange cloning vector pBBR1MCS, carrying different antibiotic resistance cassettes. Gene 166:175–176. https://doi.org/10.1016/0378-1119(95)00584-1.
50. Bradford MM. 1976. A rapid and sensitive method for the quantitation of microgram quantities of protein utilizing the principle of protein-dye binding. Anal Biochem 72:248–254. https://doi.org/10.1016/0003-2697(76)90527-3.
51. Quandt J, Hynes M. 1993. Versatile suicide vectors which allow direct selection for gene replacement in gram-negative bacteria. Gene 127:15–21. https://doi.org/10.1016/0378-1119(93)90611-6.